

A Modeling Approach to Estimating Skidding Costs of Individual Trees for Thinning Operations

Marco A. Contreras and Woodam Chung

ABSTRACT

Thinning is a common silvicultural treatment used for different forest management purposes. Traditionally, thinning prescriptions are derived from sample plots and applied to stands with various vegetation conditions. A few studies have optimized cut-tree selection to create site-specific thinning prescriptions. However, these studies greatly simplify the estimation of harvesting costs by ignoring the location of the cut trees relative to the extraction point. Consequently, resulting tree-level thinning prescriptions might not provide the most economically efficient selection of cut trees. In this study, we developed a model to estimate skidding costs of individual cut trees based on size, location, and spatial distribution of selected cut trees. The model uses a log-bunching algorithm to identify log-pile locations and then creates a skid-trail network that connects log piles to the exit point at a minimum skidding cost. We applied the model to a treatment unit, where light detection and ranging data were used to obtain terrain and tree data, considering two thinning scenarios with target densities of 400 and 300 leave trees/ha, respectively. Comparison of the model results with those obtained from the existing cost models indicates that our model results are within a reasonable range for skidding costs. As our model considers terrain slope to create skid trails, it can be effectively used to delineate nonaccessible or difficult terrain areas for skidding operations. The model can also be used to automatically generate optimal skid-trail networks connecting multiple log piles to the exit point.

Keywords: selective harvesting, skid-trail networks, forest operations, forest management, LiDAR

Thinning is a common silvicultural treatment used for different purposes in forest management. It has been used for many decades to increase tree growth for timber production (Brodie et al. 1978, Barbour et al. 1994, Bailey and Tappeiner 1998), to lower the risk of high-intensity wildfires by reducing fuel loads (Graham et al. 1999, Pollet and Omi 2002, Agree and Skinner 2005), and, increasingly in the last decade, to modify stand structure and introduce spatial heterogeneity for wildlife habitat improvement (Hayes et al. 1997, Carey 2001).

Independent of treatment objectives, thinning prescriptions are traditionally developed from ground sample plots. However, because sample plots do not usually capture the full range of variability in terrain and vegetation within each stand, thinning prescriptions might not produce the most desirable results when extrapolated and applied to multiple stands with different site potentials and vegetation structures (Pukkala and Miina 2005). Efforts to develop site-specific thinning prescriptions by optimizing cut-tree selection at the individual-tree level have yielded two approaches: the first one formulates the cut-tree selection process as a nonlinear problem and solves it using the Hooke and Jeeves (1961) algorithm (Valsta 1992, Pukkala and Miina 1998), whereas the other approach uses an integer-programming model (Hof and Bevers 2000). Several studies have used the former approach to develop thinning prescriptions that maximize the economic return on different forest types (Rautiainen et al. 2000, Palahí and Pukkala 2003, Hyytiäinen et al. 2005, Cao et al. 2006). However, when considering the economics of thinning operations, all of these studies greatly simplify the estimation

of harvesting costs by using average values of stand attributes, such as skidding distance, ground slope, and harvest volume, while ignoring the location of the individual cut trees relative to exit points (either road side or log landing). Consequently, tree-level thinning prescriptions developed by these past studies might not provide the most economically efficient selection of cut trees. In addition, these approaches for optimal tree selection have been applied to only sample plots. Their application to entire stands has been limited because of a lack of individual tree-level information.

Recently, new remote sensing and geographic information systems (GIS) technologies such as light detection and ranging (LiDAR) have been used to provide inventory data at the individual tree level. For example, tree heights, crown widths, and derivative parameters, such as dbh and volume, are some of the tree characteristics that have been derived from LiDAR data (Maltamo et al. 2004, 2006, Packalén and Maltamo 2006). As this type of high-resolution spatial data becomes more available, there is increasing potential to use optimal tree selection algorithms to develop site-specific, tree-level thinning prescriptions that can be applied to an entire stand (Shao and Reynolds 2006). However, harvesting cost models that provide estimates for individual cut trees still need to be developed and implemented into optimal tree selection algorithms to ensure cost efficiency of thinning operations for given management purposes.

In this study, we present a computerized model to develop skid trail networks and estimate tree-level timber harvesting costs. The model considers size, location, and spatial distribution of individual

Manuscript received October 12, 2009, accepted March 8, 2011.

Marco A. Contreras (marco.contrerasalgado@umontana.edu) and Woodam Chung, Department of Forest Management, University of Montana, 32 Campus Drive, Missoula, MT 59812. We thank Dr. Carl Seiestad for providing LiDAR data for the study area.

This article uses metric units; the applicable conversion factors are: centimeters (cm): 1 cm = 0.39 in.; meters (m): 1 m = 3.3 ft; cubic meters (m³): 1 m³ = 35.3 ft³; kilometers (km): 1 km = 0.6 mi; hectares (ha): 1 ha = 2.47 ac.

Copyright © 2011 by the Society of American Foresters.

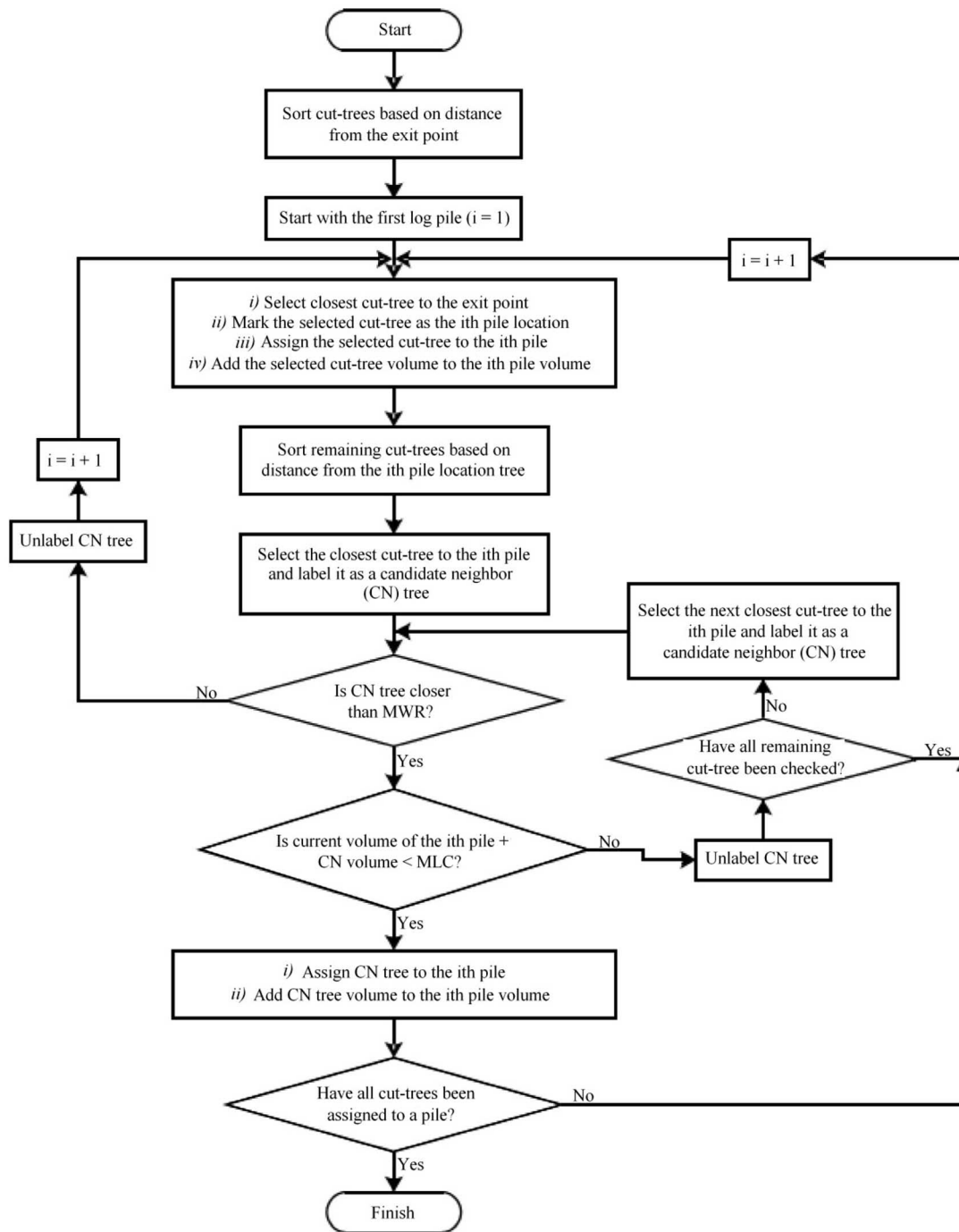


Figure 1. Flow chart of the log-bunching algorithm developed in this study. MWR, maximum winching radius; MLC, maximum loading capacity.

cut trees and is designed for ground-based harvesting operations. If coupled with optimal cut-tree selection algorithms, this model is expected to develop cost-efficient thinning guidelines for given treatment objectives.

Methodology

A treatment unit is defined in this study as an area to be thinned by a ground-based harvesting system. All logs are assumed to be brought into one exit point (log landing), where they are loaded onto log trucks for further transportation. A whole-tree harvesting is further assumed for this study as follows: (1) cut trees are felled at the

stump location, (2) a cable skidder is used to bunch and skid nearby cut trees within a maximum winching radius (MWR) to a given log landing, and (3) trees are then delimbbed and topped at the landing.

This study is based on the availability of a stem map, preselected cut- and leave-tree locations, and terrain information within the entire treatment unit. For this study, a stem map and a digital elevation model (DEM) derived from LiDAR data by Rowell et al. (2009) was used. In their study, the LiDAR raw data were processed to produce a high-resolution 1-m DEM and a canopy height model. Tree locations were obtained using a stem identification algorithm based on a combination of variable window local maxima filtering

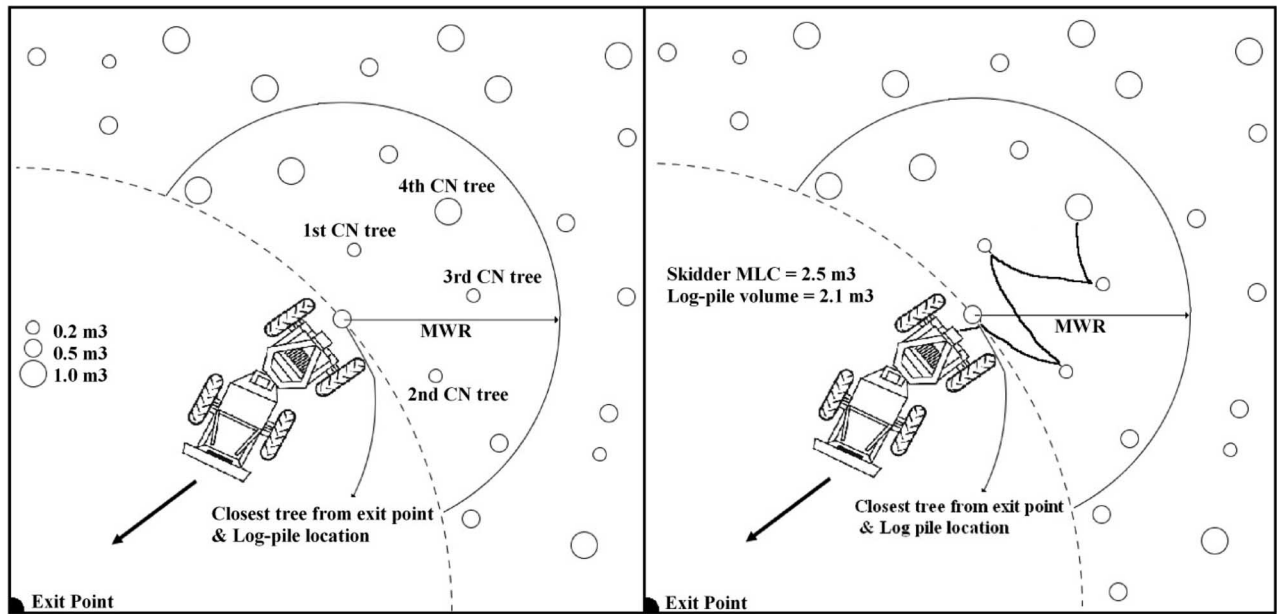


Figure 2. Log-bunching simulation to identify log-pile locations. CN, candidate neighbor; MWR, maximum winching radius; MLC, maximum loading capacity.

(Popescu and Wynne 2004) and neighborhood canopy height variance and return density (Rowell et al. 2006). Individual-tree dbh were estimated using a log-linear model ($n = 1555$, $R^2 = 0.76$, error = 7.6%) (Rowell et al. 2009):

$$\ln \text{ dbh} = 1.732 + (0.041 \times h) + (0.798 \times \text{rh}) - (0.007 \times \text{sd}), \quad (1)$$

where h is the height of the tree (m); rh is the relative height (m), calculated as the tree height divided by the mean height of dominant and codominant trees in a 20×20 -m neighborhood; and sd is stem density of dominant and codominant stems in the neighborhood. Tree volumes were estimated using an equation from the Northern Idaho/Inland Empire of the Forest Vegetation Simulation (Keyser 2010):

$$\text{Vol} = [\{0.00171 \times (2.54 \times d)^2 \times h\} + \{0.00171 \times (2.54 \times d) \times h\}] \times 0.02831, \quad (2)$$

where Vol is the tree volume (m^3) and d is the tree dbh (cm). This LiDAR-derived DEM and stem map, as well as the location of the exit point for the treatment unit, are the main input data sets for our cost model.

To estimate harvesting cost for individual trees, the model first uses a log-bunching algorithm to identify log-pile locations and volumes. The algorithm simulates a cable skidder operation that collects nearby cut trees through a cable winch to complete a full load and skids trees together to a landing. The target maximum loading capacity (MLC) of the skidder was used to limit the volume of a log pile that the skidder can carry during its travel to the landing, assuming log volume is the limiting factor on skidding capacity, not the number of log pieces. The model then designs the skid-trail network that connects each log-pile location to the exit point while minimizing the total skidding cost. The model estimates the skid-

ding cost for a given i th log pile (PSC_i) using

$$\text{PSC}_i = \left(\frac{\text{CT}_i}{60} \right) \times \text{RR}, \quad (3)$$

where CT_i is the skidding cycle time in minutes for a round trip between the exit point and the i th log-pile location and RR is the rental rate of the skidder in $\$/\text{hr}$. Cycle times can be estimated using regression models that appropriately capture the interaction between the skidding equipment and the terrain conditions such as slope and distance. However, there exist no regression models that accurately provide estimations of cycle time for short distances such as those obtained from a high-resolution DEM. Therefore, for demonstration purposes, we modified the skidding cycle time models introduced by Han and Renzie (2005) and used them in our model applications to estimate downhill and uphill skidding cycle times that are proportional to skidding distances (Equations 4 and 5). We also assumed that the uphill skidding cycle time is 20% greater than downhill cycle time for equal skidding distance:

$$\text{CT}_{\text{ds}} = 3.9537 + (0.0215 \times D), \quad (4)$$

$$\text{CT}_{\text{us}} = 3.9537 + (0.0258 \times D), \quad (5)$$

where CT_{ds} is the cycle time for downhill skidding, CT_{us} is the cycle time (min) for uphill skidding, and D is the skidding slope distance (m) from a given log-pile location to the treatment unit exit point.

To estimate the skidding cost of an individual tree, the model prorates the skidding cost on the basis of the volume ratio of the individual tree to the entire log pile (Eq. 6). Thus, bigger cut trees entail a larger skidding cost than smaller cut trees in the same pile:

$$\text{TSC}_j = \left(\frac{\text{vol}_j \times \text{PSC}_i}{\text{Pvol}_i} \right), \quad (6)$$

where TSC_j is the skidding cost of the j th individual cut tree, vol_j is the volume of the j th cut tree, PSC_i is the skidding cost of the i th log pile containing cut tree j , and Pvol_i is the volume of the i th log pile.

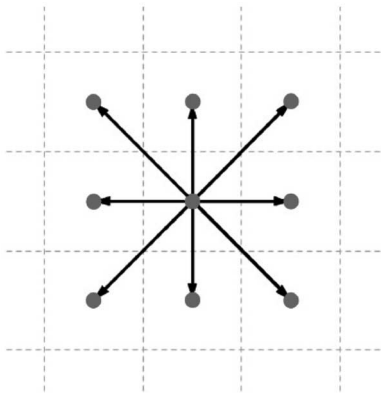


Figure 3. Links connecting a cell with its eight adjacent cells.

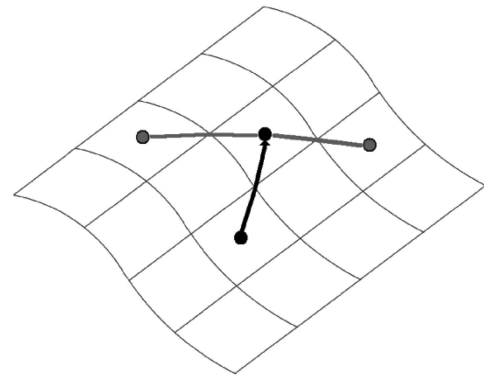


Figure 4. Grid cells used to calculate the side slope and skid-trail gradient for a given skid-trail link.

Log-Bunching Algorithm

The log-bunching algorithm identifies the number, volume, and location of log piles based on the three-dimensional coordinates of each cut tree provided by the DEM and stem map. Figure 1 shows a flow chart describing the log-bunching process. The process begins with sorting all cut trees based on their slope distance from the treatment unit exit point. Starting with the first log pile ($i = 1$), the algorithm selects the closest cut tree to the exit point. This closest cut tree is identified as the i th log-pile location (Figure 2), assigned to the log pile, and its volume is added to the i th log pile. After the i th log-pile location has been identified, the algorithm re-sorts all remaining unassigned cut trees based on their slope distance from the

i th log pile. The closest cut tree to the i th log pile is selected and labeled as a candidate neighbor (CN) cut tree to be added to the log pile. If the CN cut tree is beyond the MWR, the algorithm stops assigning cut trees to the i th log pile, the current CN cut tree is unlabeled, and the process continues for the next pile ($i = i + 1$). If the CN cut tree is within the MWR, the algorithm checks whether the current volume of the i th log pile plus the CN cut-tree volume exceeds the MLC of the skidder. If the combined volume is greater than the MLC, the current CN cut tree is unlabeled and the next closest cut tree to the i th log pile is selected and labeled as a CN cut tree. On the other hand, when the combined volume is less than the

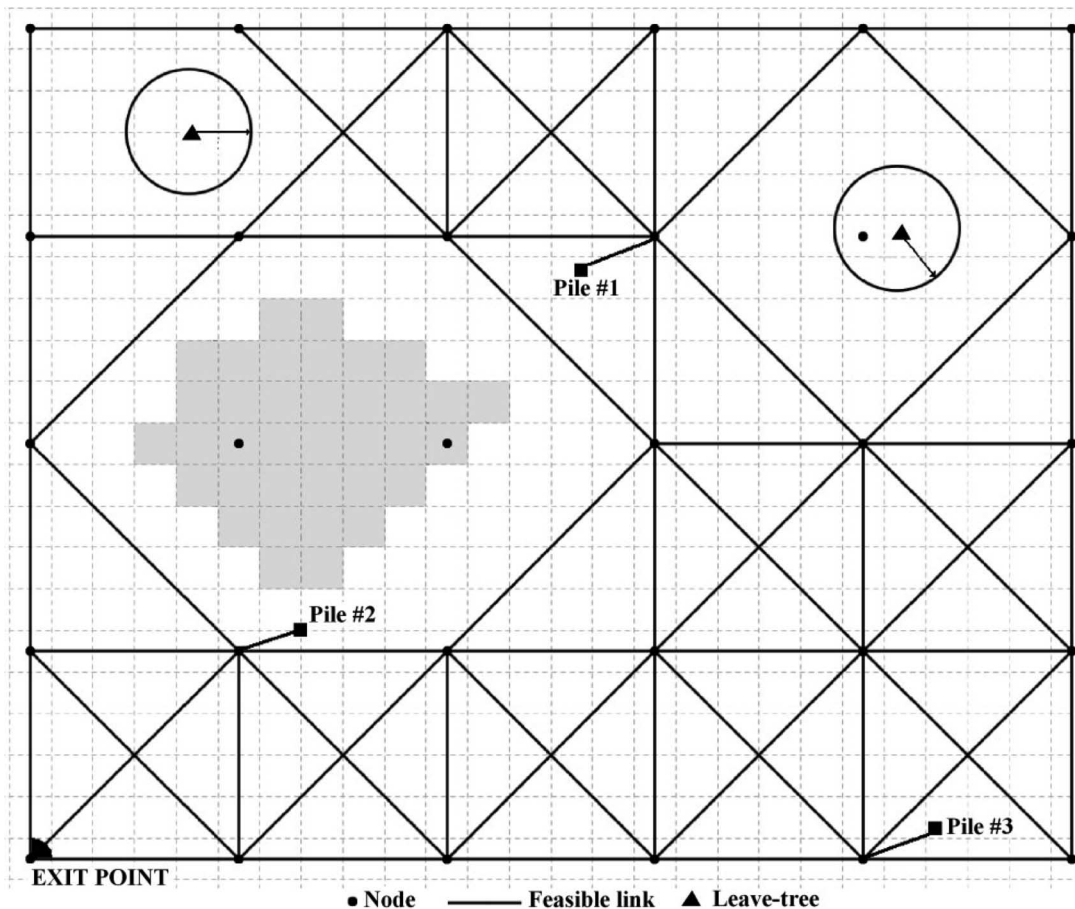


Figure 5. Example of the skid-trail network created over an area with steep terrain and obstacles presented by two leave-tree buffers.

MLC of the skidder, the CN tree is assigned to the i th log pile and the pile volume is updated. When no more cut trees can be assigned to the i th log pile because of MLC, the algorithm moves to the next ($i = i + 1$) log-pile location. Figure 2 shows a log-bunching example for a log pile including five cut trees with a combined volume of 2.1 m^3 , when the MLC is 2.5 m^3 . The algorithm stops the log-bunching process when all cut trees in the treatment unit have been assigned to a log pile.

Skid-Trail Network

To estimate the skidding cycle time for a given log pile, it is necessary to know the route the skidder will follow between the log-pile location and the treatment unit exit point. Our model identifies the route that connects each log pile to the exit point at a minimum cycle time. To determine the least cycle time route location, the model creates a skid-trail network consisting of a set of nodes and links. Nodes represent the center of DEM grid cells, log-pile locations, and the treatment unit exit point, and links represent connections to adjacent nodes (Figure 3). In our model, each node is connected to its eight adjacent neighbors. A skid-trail network generated from all possible nodes in the 1-m DEM has a very large number of nodes and links even for a small treatment unit. To reduce the size of the problem of finding minimum cycle time routes, we created a skid-trail network with nodes spaced at 5 m.

Before creating a link, the model checks whether skidder traffic is feasible over the link representing a skid-trail segment. Typically, for safety and productivity reasons, skidder operations are limited to areas with gentle slopes. Therefore, a link is only created when the link gradient and side slopes are both below a predefined maximum skid-trail gradient (MSTG) and maximum skid-trail side slope (MSTSS). Skid-trail gradient is calculated based on the elevation difference of the two cells forming the link (solid line in Figure 4). Side slope is calculated on the basis of the elevation difference and horizontal distance between the two grid cells of the front grid cell of a link (shaded line in Figure 4). To avoid damage to the residual stand, we set a safety buffer distance (SBD) for each leave tree in the treatment unit where no skid trails are allowed to pass through. Figure 5 shows an example of a skid-trail network on an area with three pile locations, steep terrain (shaded grid cells in Figure 5), and obstacles presented by leave trees. Any other zones where heavy machinery traffic should be limited, such as wetlands or unstable soils, can be specified and included in the model.

After the skid-trail network has been created, the model estimates the variable cycle time associated with each link. We assumed that the first term in Equations 4 and 5 is an estimate of the fixed cycle time due to activities such as hooking and unhooking logs to the winch line, and the second term estimates the skidder travel time on a skid-trail. Thus, because the fixed cycle time is independent of the skid-trail route location, the model estimates the variable cycle time for each link using only the second term in Equations 4 and 5.

Once the variable cycle time is calculated for each link, a network problem is formulated to find a set of routes that has the least variable cycle time from each log-pile location to the treatment unit exit point. The variable cycle time per link is used as the link attribute value, and the objective function is to minimize the total variable cycle time. The model uses Dijkstra's shortest path algorithm (Dijkstra 1959) to find the set of routes connecting each log pile to the exit point with the least variable cycle time and then estimate the total variable cycle time for each log pile. The shortest path algo-

rithm used in the model is known to be efficient and is widely used to determine the shortest paths between a destination node and a set of origin nodes in a given network (Tan 1999, Anderson and Nelson 2004, Chung et al. 2004).

Once the minimum variable cycle time route has been found for a given log pile, the model adds the fixed cycle time (first term in Equations 4 and 5) to obtain the total cycle time for the log pile (CT in Equations 4 and 5). CT is then used to compute the skidding cost for the pile and estimate skidding cost of individual cut trees included in the log pile.

Model Application: A Case Study

We applied our model to a treatment unit in the University of Montana's Lubrecht Experimental Forest, located approximately 48 km northeast of Missoula, Montana, in the Blackfoot River drainage. The treatment unit is 4.6 ha in size, with elevations ranging from 1,270 to 1,310 m and an average slope of 13.5% (0.0–36.3% slope range) (Figure 6a). For the purpose of fuel reduction, we considered a thinning prescription that cuts, piles, and burns all trees with dbh less than 12.7 cm (5 in.) and selects and harvests some merchantable trees for cost recovery. The LiDAR-derived stem map identified 2,645 individual stems with a dbh larger than 12.7 cm. Figure 6b shows the locations of these trees in the treatment unit.

The selection of leave trees (and thus cut trees) in the treatment unit was done manually, simulating the marking process carried out by markers on the ground based on tree sizes and spacing between trees. Because of residual stand protection requirements, skid trails within the SBD of any leave tree are not allowed. Thus, depending on the number and location of leave trees, the resulting skid-trail network might not be fully connected, leaving piles isolated from the exit point. In this situation, we assumed that the isolated piles are left on the site without being skidded to the landing.

We considered two thinning intensities scenarios to explore the performance of our cost model. For scenario I, cut trees were selected from the treatment unit (see Figure 6b) until a target tree density of 400 leave trees/ha was met. For scenario II, additional cut trees were selected among the trees left by scenario I until a target tree density of 300 leave trees/ha was met. Figure 7a and 7b shows the locations of the leave tree for scenarios I and II, respectively. Table 1 shows the number of cut and leave trees, average spacing between trees, and target cut and leave volume on the treatment unit after both selective harvesting scenarios are simulated.

The cost model was applied to the treatment unit for both scenarios considering the following link feasibility parameters: SBD = 1.5 m, MSTG = 35%, and MSTSS = 35%. The model also considered the following harvesting equipment parameters: MLC = 2.5 m^3 , RR = 85 \$/hr, and MWR = 10 m, which approximately correspond with a small cable skidder used in thinning operations (Bustos-Letelier 2010). The exit point was located on the lower-elevation part of the treatment unit (see Figure 6a).

Results and Discussion

The model identified log-pile locations, as well as the optimal skid-trail network connecting log piles to the treatment unit exit point for both simulated selective harvesting scenarios. For scenario I, based on the location of the 805 selected cut trees (Figure 8a), the log-bunching algorithm identified a total of 215 log-pile locations (Figure 8b). Then, based on the location of the 1,840 leave trees and

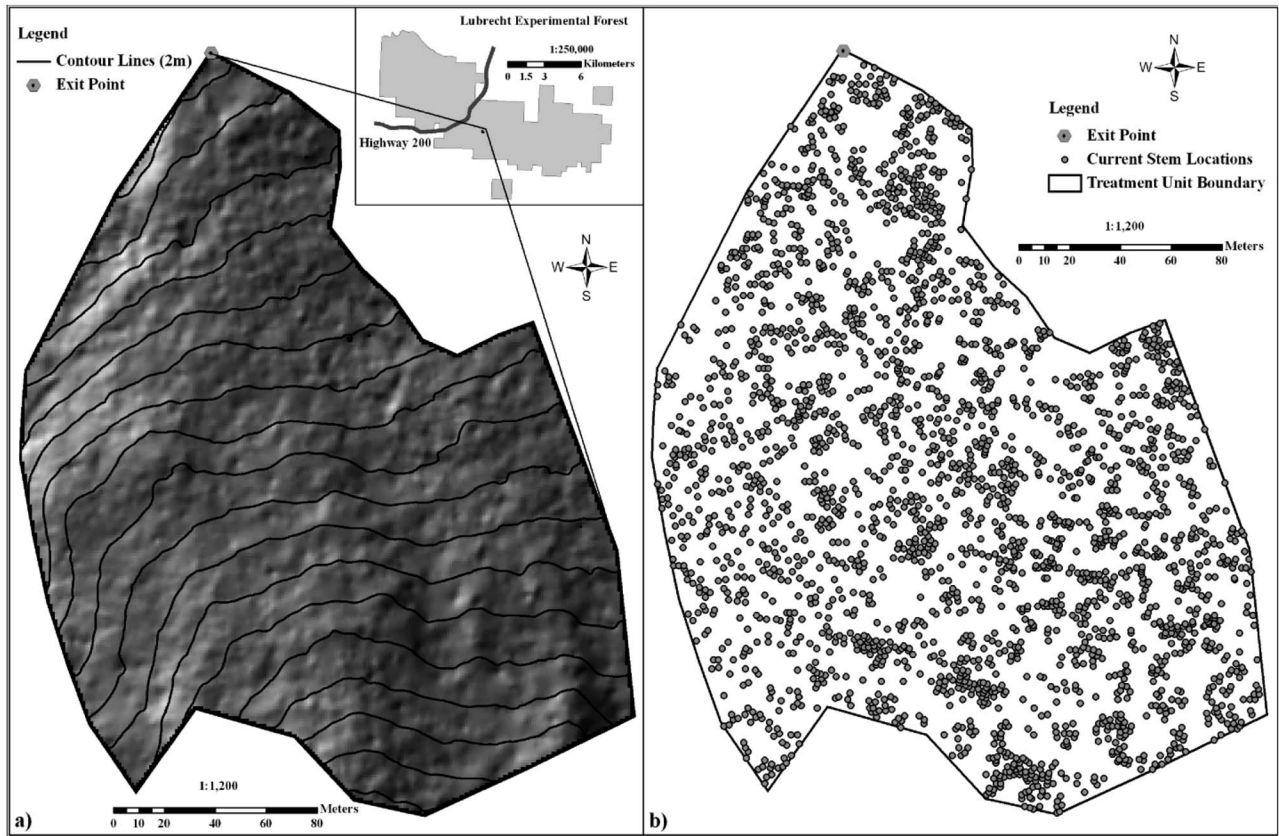


Figure 6. Light detection and ranging-derived digital elevation model (a) and stem map (b) for the treatment unit selected for the model application area in the Lubrecht Experimental Forest.



Figure 7. Leaf-tree locations after manually selected cut trees were removed under the two thinning scenarios, with target densities of 400 (a) and 300 (b) trees/ha.

Table 1. Target thinning intensities under each thinning scenario considered in the study.

Target conditions	Scenario I (400 trees/ha)	Scenario II (300 trees/ha)
Number of leave trees	1,840	1,380
Number of cut trees	805	1,265
Average tree spacing (m)	5.0	5.8
Leave volume (m ³)	573.74	406.58
Cut volume (m ³)	200.32	367.48

the identified log piles, the model created a skid-trail network composed of 2,710 feasible skid-trail links between nodes. Figure 9a shows the skid-trail network, where the model identified 11 of the 215 log piles as isolated without a way out to the exit point, and considered the cut trees belonging to these log piles as nonharvestable. These isolated log piles are caused mainly by the leave-tree buffers, where no skidder access is allowed. For the remaining 204 connected piles, the model determined the optimal skid-trail network that minimized the variable cycle time from each log pile to the exit point (Figure 9b). Figure 10a and 10b presents the optimal skid-trail network with traffic levels on each skid-trail link in terms of timber volume and number of passes (turns). The model estimated the skidding costs for each connected log pile using the variable cycle time obtained from the optimal skid-trail network. Figure 11a shows range of skidding costs per log pile, where log piles located farther away from the exit point have larger harvesting costs. The model also estimated skidding costs for individual cut trees (Figure 11b). Cut trees with large cost can be found throughout the

treatment unit because cost is a function of both distance from the exit point and individual cut-tree volume.

For scenario II, which considered 1,265 cut trees (Figure 12a), the log-bunching algorithm identified 278 log-pile locations (Figure 12b). The model created a skid-trail network composed of 3,414 feasible skid-trail links (Figure 13a). Because of the smaller number of obstacles presented by fewer leave trees, there were no isolated log piles identified by the model. Using the variable cycle time of each link, the model determined the optimal skid-trail network connecting each log pile to the exit point at a minimum cycle time (Figure 13b). The optimal skid-trail network, showing traffic levels in terms of volume traveled and the number of passes, is presented in Figure 14a and 14b. The model also estimated the skidding costs of the 278 log piles, as well as skidding costs of the 1,265 individual cut trees in the treatment unit (Figure 15a and 15b). Similar to scenario I, log piles located closer to the exit point have smaller skidding costs than distant log piles.

Table 2 summarizes the model results for both harvesting scenarios. As mentioned above, a total of 55 cut trees (6.8% of the total selected cut trees) were identified as nonharvestable in scenario I mainly because of leave-tree buffers. However, the combination of other factors related to the harvesting equipment and skid-trail network design can also affect the number and location of isolated log piles. For example, MLC and MWR influence the number of cut trees included in a log pile, thus affecting the number and location of log piles. Likewise, the spacing between nodes can also determine whether a log pile is either connected to the network or isolated. In our model, a log-pile location is defined as the location of the closest

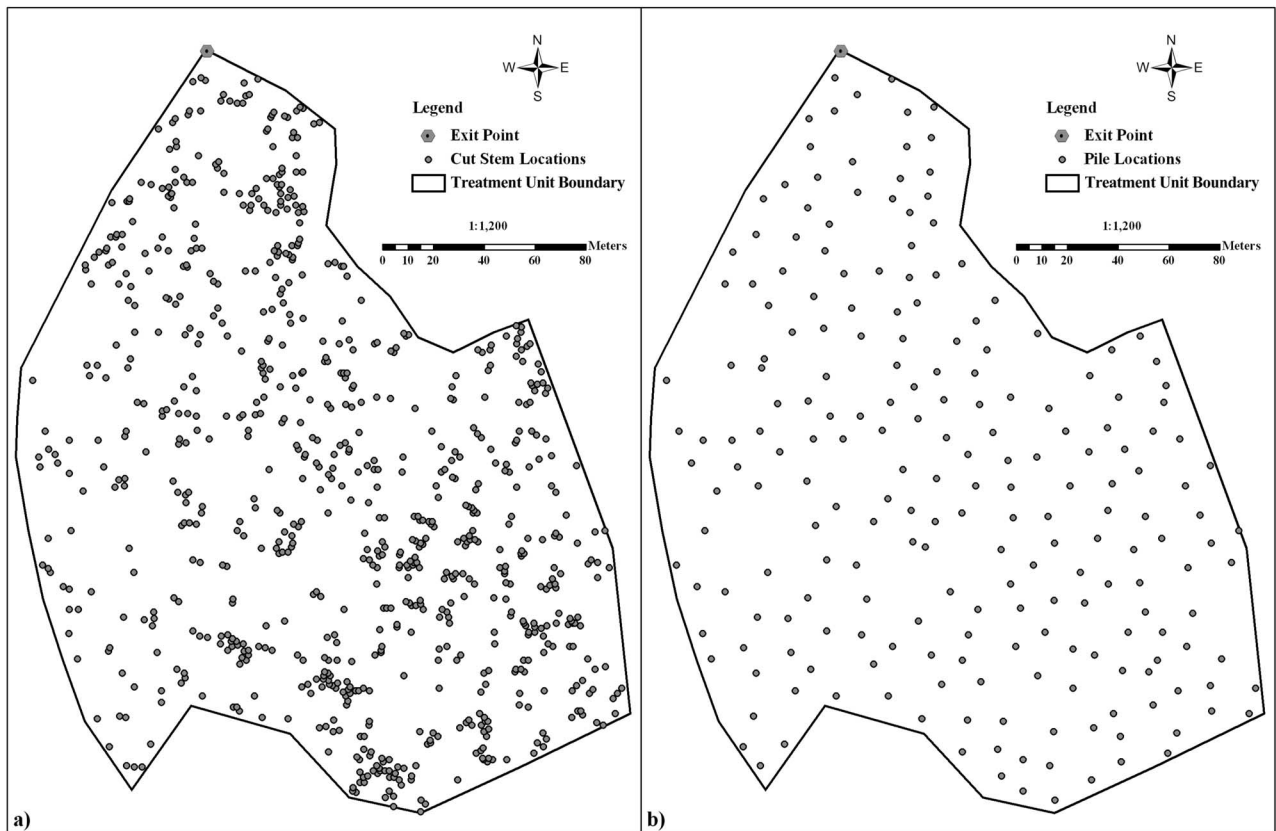


Figure 8. Cut-tree locations under thinning scenario I (a) and the corresponding log-pile locations identified by the log-bunching algorithm (b).

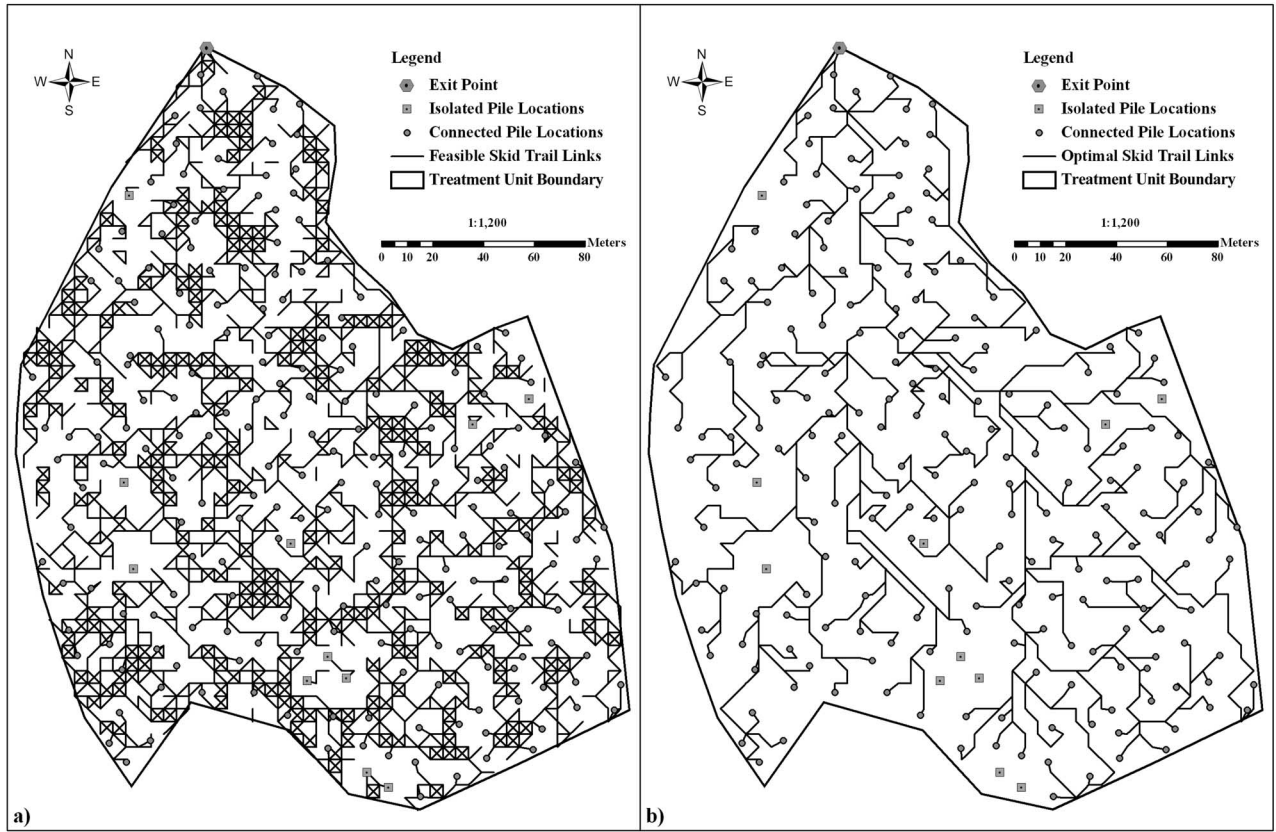


Figure 9. Feasible skid-trail links created by the model for thinning scenario I (a) and the optimal skid-trail network identified by the model (b).

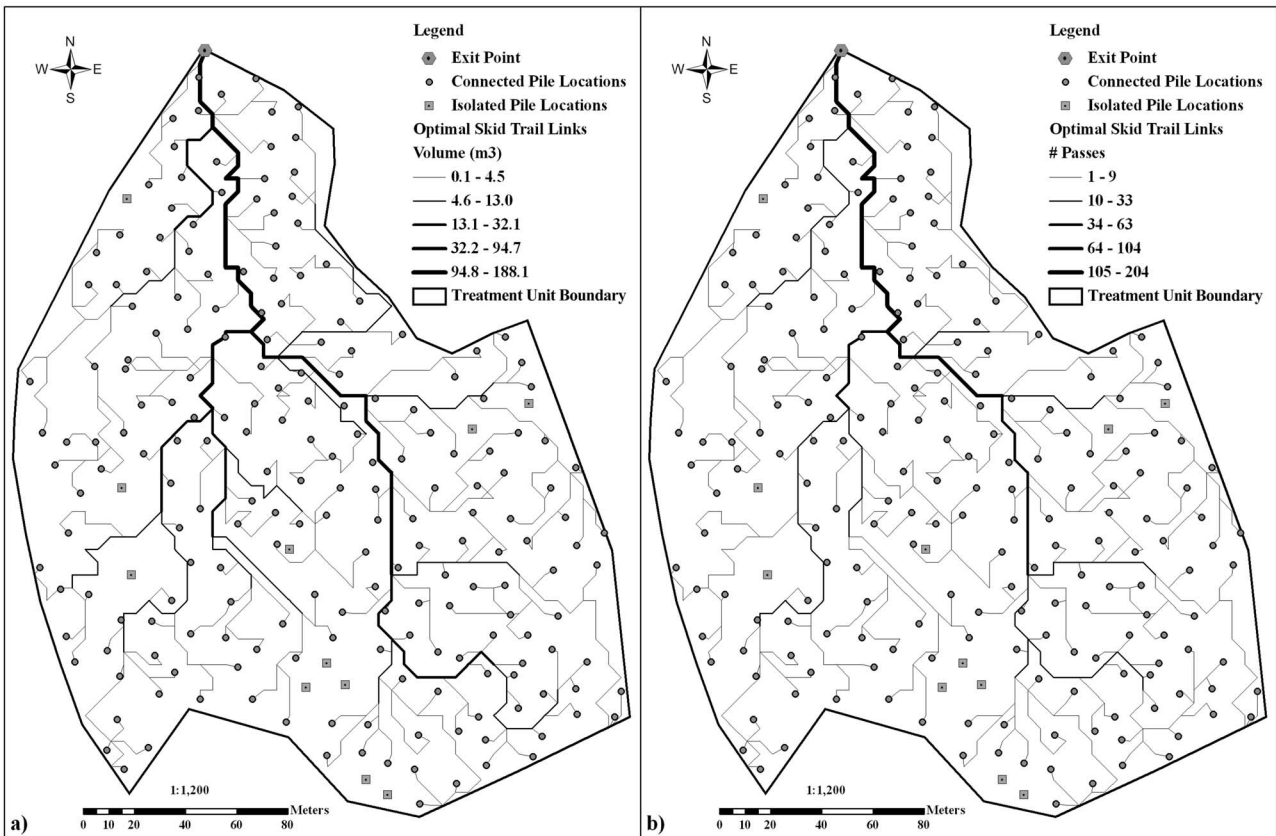


Figure 10. Optimal skid-trail network for thinning scenario I showing traffic levels in terms of volume traveled (a) and number of passes (b) over a given link.

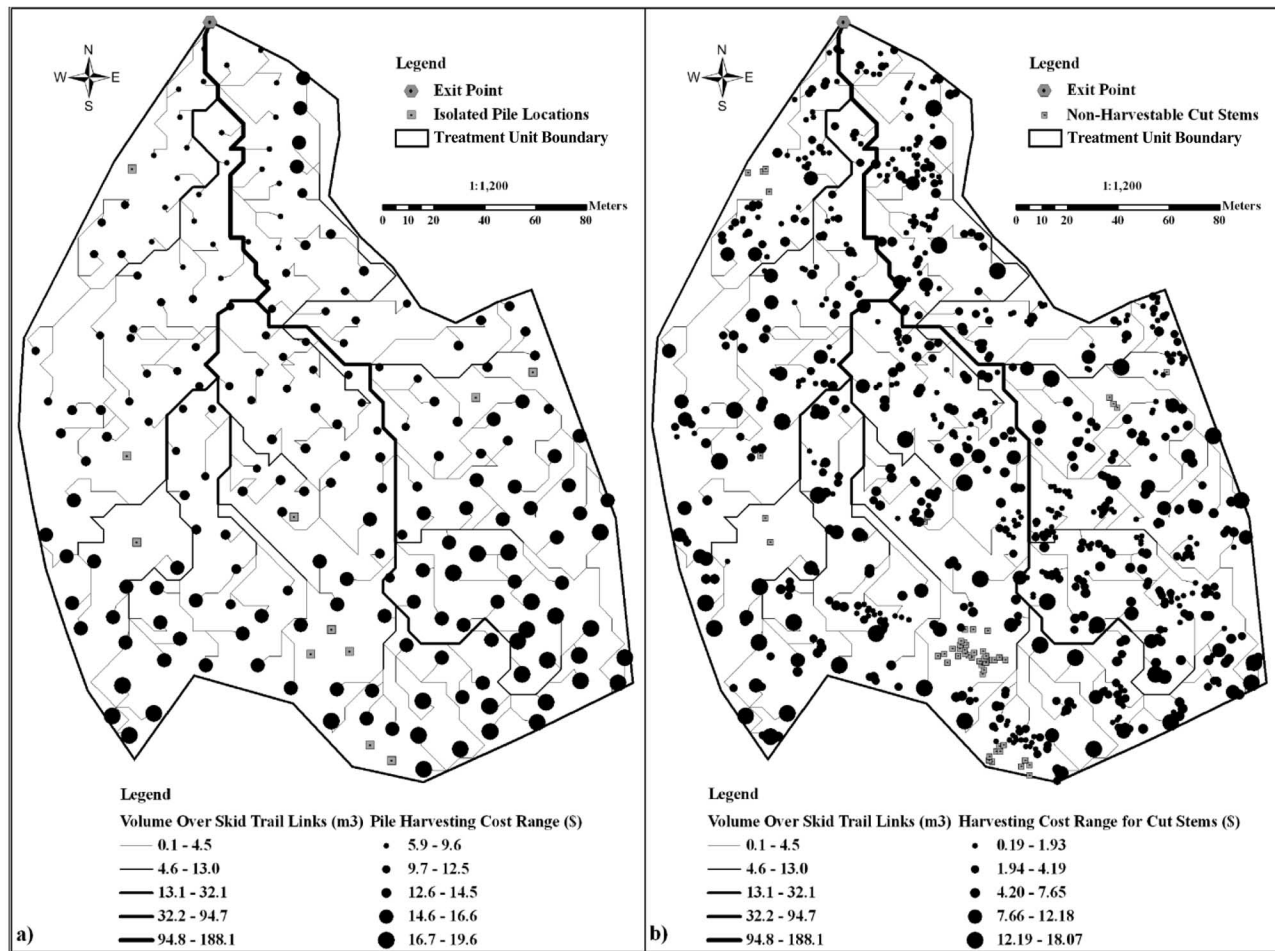


Figure 11. Model results showing skidding cost per pile (a) and per individual cut-tree (b) for thinning scenario I.

available cut tree to the exit point, and if its location is within a leave-tree SBD, then the log pile and all cut trees forming it are considered isolated. However, in practice, cut trees inside a leave-tree SBD can be winched out of the no-traffic zone and the log-pile location can be shifted, allowing these isolated trees to be extracted. Our model will need to be further refined to reflect this practical aspect of log piling. In addition, leave trees were selected on the basis of tree sizes and spacing; however, if access is considered when selecting leave trees, the number of isolated log piles identified by the model in this study can be significantly reduced, thus increasing timber recovery.

Log-pile characteristics between the two scenarios were slightly different. The average number of trees per log pile is smaller for scenario I than for scenario II (3.7 versus 4.6) because fewer trees are available within the MWR to complete a full load. For the same reason, scenario I had a smaller average volume per log pile than scenario II (0.92 m³ versus 1.32 m³). The maximum number of trees per log pile is relatively high in both scenarios (i.e., 11 and 15 trees) because of the large number of small trees in the treatment unit. In this study, we did not restrict the number of trees per log pile, which could be included as another limiting factor on the carrying capacity of cable skidders. In addition, because tree size was not considered in the cycle time equations (Equations 4 and 5), our skidding cost estimates are independent of tree size. However, because small trees require more piling time than large trees to complete a full load, reducing

tree sizes typically results in increases skidding costs per cubic meter. Further research should consider evaluating skidding cycle time equations that account for such factors to obtain more realistic skidding cost estimates. The average distance from a log pile to the exit point was approximately 260 m and 225 m for scenarios I and II, respectively. The higher average distance for scenario I was caused by the presence of more leave trees, which present obstacles to skidding paths. Because of this longer skidding distance in scenario I, the average skidding cost in scenario I is slightly higher than scenario II (\$13.6 versus \$12.5). Likewise, the average skidding cost for individual cut trees is higher in scenario I than scenario II (\$3.46 versus \$2.75).

To ensure that our model results are comparable to those that can be obtained from the existing skidding cost models, we first aggregated the individual tree skidding costs estimated from the application results described above to calculate the average skidding cost per unit of timber volume (\$/m³). The average cost was then compared with average skidding costs estimated by conventional cost regression models that use average values of stand attributes (i.e., harvest volume per ha, average skidding distance, etc.) as explanatory variables.

For this comparison, we selected the Fuel Reduction Cost Simulator (FRCS) (Hartsough et al. 2001) that is currently used as timber harvest cost estimator for multiple Microsoft Excel-based tools, such as STHARVEST (Fight et al. 2003) and My Fuel Treatment Planner (Biesecker and Fight 2006). We compared our model

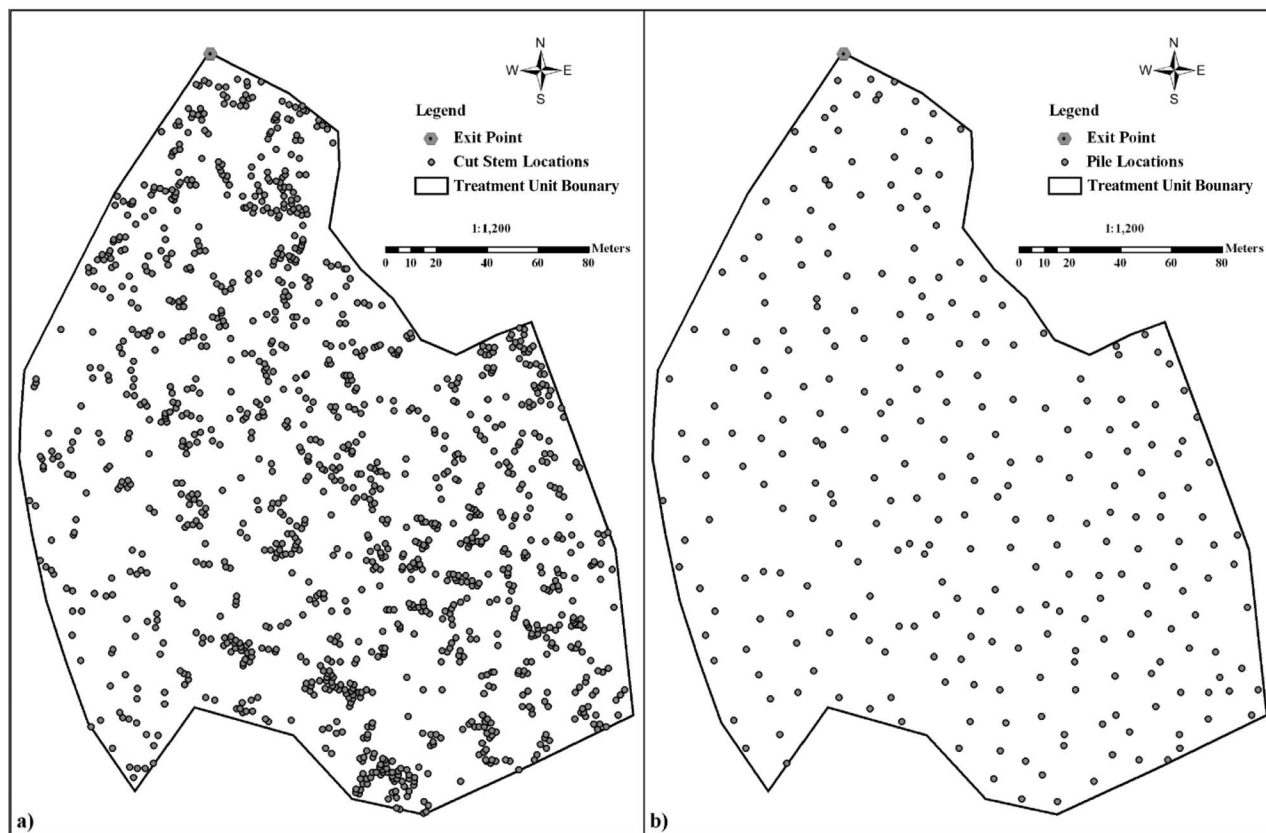


Figure 12. Cut-tree locations under thinning scenario II (a) and the corresponding log-pile locations identified by the log-bunching algorithm (b).

results with the skidding cost component of FRCS, which is calculated as a weighted average of skidding costs estimated by six published regression models. These regression models were developed for cable skidders of various sizes operating in different areas of the western United States, such as western Montana, Idaho, Oregon, and Washington (Gebhardt 1977, Gardner 1979, Johnson 1998). The skidder rental rate, cut-tree characteristics, and thinning intensities entered into FRCS as input parameters were the same as those used in our model applications. The average skidding distance (ASD) calculated as the slope distance from the centroid of the treatment unit to exit point. Other characteristics of the treatment unit, such as size and average slope, were also entered into FRCS (Table 3).

Table 4 summarizes cost estimates resulted from our individual tree skidding cost model, FRCS, and the six cost regression models used in FRCS for both thinning scenarios. The skidding costs from our model are about 33% higher and 5% lower than the FRCS cost estimates for scenarios I and II, respectively. However, our model results are within the range of estimates produced by the six regression models. All models estimated skidding costs of scenario I higher than scenario II, but the difference between the two scenarios was larger in the results of our model than in those of the existing models, which indicates that our cost model is more sensitive to thinning intensities than the existing models. This is mainly because thinning intensity does not affect ASD used in the existing models considered, whereas in our model, ASD is calculated as the average distance from all log piles to the exit point along the optimal skid-trail network. However, modern skidding cost models should consider thinning prescriptions to better capture the interactions be-

tween thinning intensity and skidding operations and obtain more realistic estimates of the associated skidding costs.

Although our model provides reasonable average cost estimates ($\$/m^3$) compared with traditional methods, the accuracy of individual-tree cost estimates largely depends on the accuracy of the input tree locations. There are several ways to obtain stem map information, from traditional field measurements to advanced remote sensing and GIS technologies, such as high-resolution aerial photo (Hirschmugl et al. 2007), multispectral imaging (Popescu and Wynne 2004), and LiDAR (Maltamo et al. 2004). The algorithms used to derive LiDAR-derived stem maps in our study area have provided stem detection accuracies of approximately 53% when considering all forest types (Suratno et al. 2009). However, stem detection accuracy increases significantly on dominant trees. In forest conditions similar to those of our treatment unit, the stem detection algorithm provided an accuracy of about 90% when considering only dominant trees (Rowell et al. 2006). In this study, we considered only dominant trees with dbh >12.7 cm; thus, we expect that the stem map used for our study has a high level of stem detection accuracy.

As our model considers terrain slope to create feasible skid-trail links, it can be effectively used to delineate nonaccessible or difficult terrain areas for skidding operations. Our model can also be used to automatically generate optimal skid-trail networks connecting multiple log piles to the exit point. In addition, soil recovery costs associated with amelioration of soil disturbances caused by skidder traffic can also be incorporated into our model to generate skid-trail networks that minimize both skidding costs and soil disturbances (Contreras and Chung 2009).

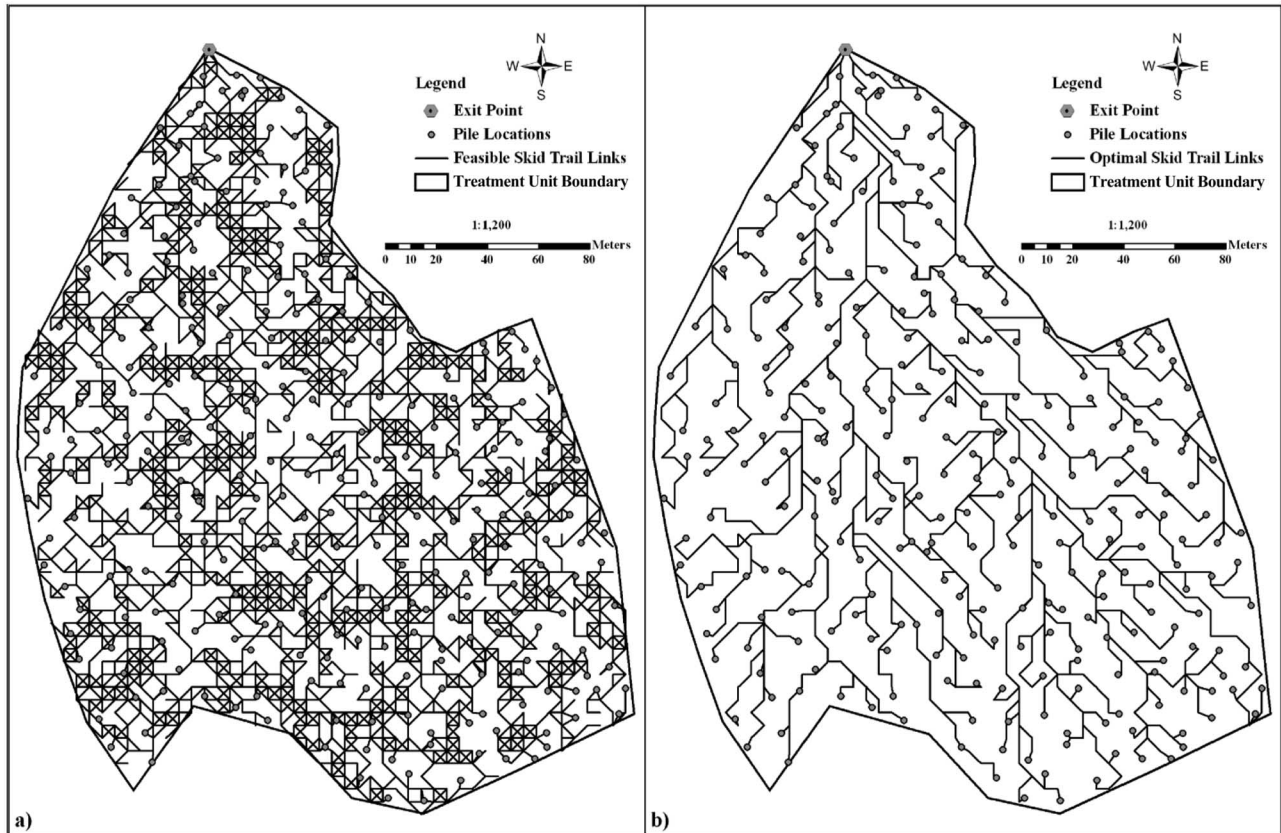


Figure 13. Feasible skid-trail links created by the model for thinning scenario II (a) and the optimal skid-trail network identified by the model (b).

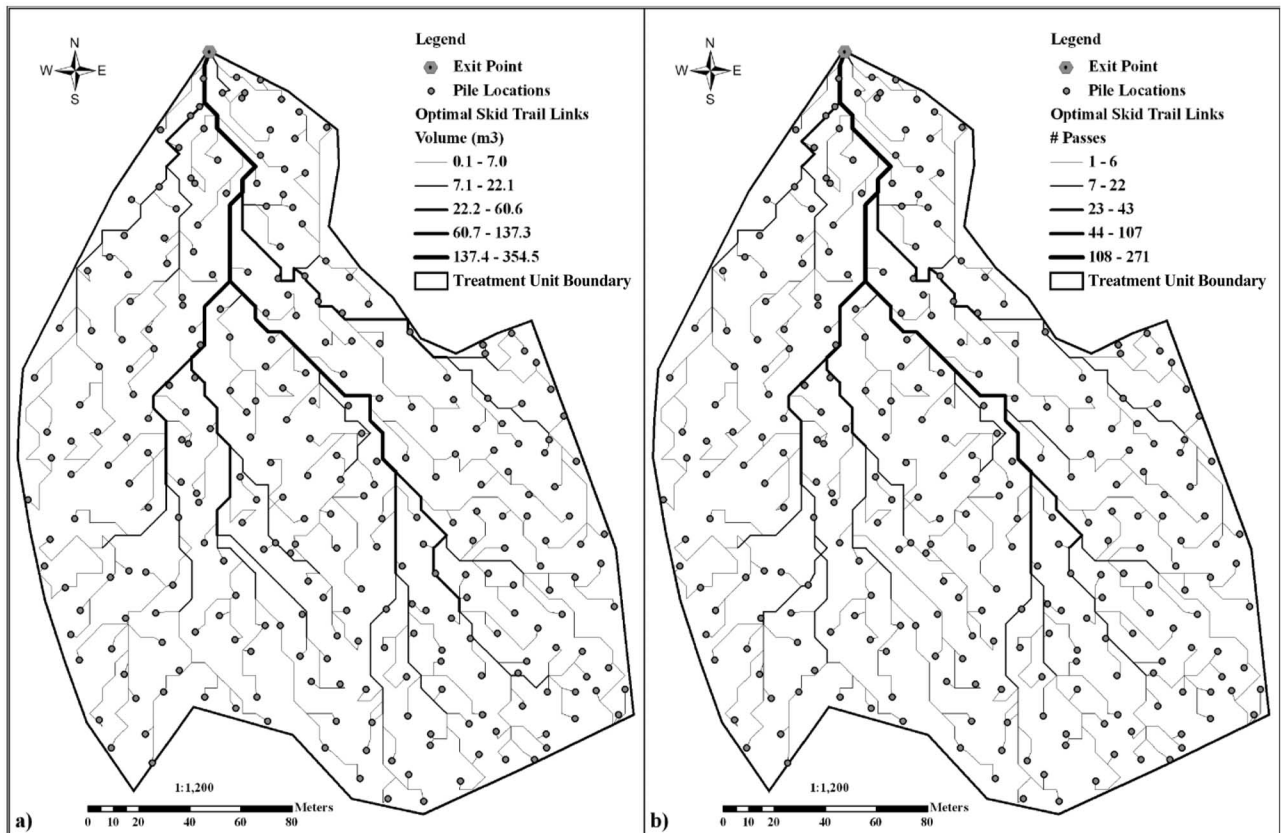


Figure 14. Optimal skid-trail network for thinning scenario II showing traffic levels in terms of volume traveled (a) and number of passes (b) over a given link.

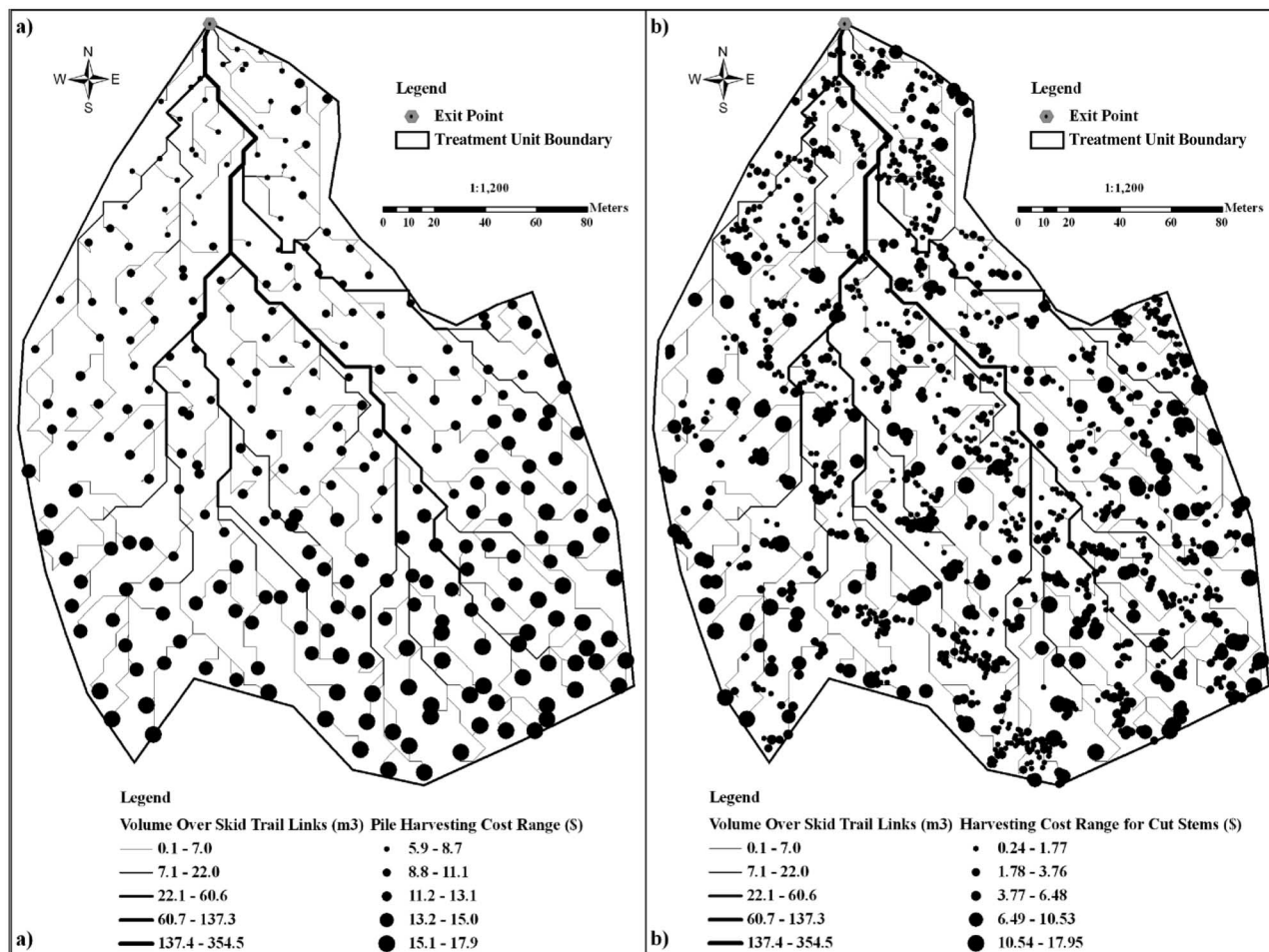


Figure 15. Model results showing skidding cost per pile (a) and per individual cut-tree (b) for thinning scenario II.

Table 2. Results of the individual tree skidding cost model applied to a treatment unit in Lubrecht Experimental Forest.

Model results	Scenario I (400 trees/ha)	Scenario II (300 trees/ha)
Harvesting feasibility		
Harvestable piles	204	278
Harvestable cut trees	750	1265
Harvestable volume (m ³)	188	367
Nonharvestable piles	11	
Nonharvestable cut trees	55	
Nonharvestable volume (m ³)	12.3	
Harvestable piles		
Minimum number of trees per pile	1.00	1.00
Average number of trees per pile	3.70	4.60
Maximum number of trees per pile	11.00	15.00
Minimum pile volume (m ³)	0.05	0.05
Average pile volume (m ³)	0.92	1.32
Maximum pile volume (m ³)	2.48	2.64
Minimum pile distance (m)	11.11	11.11
Average pile distance (m)	259.13	225.15
Maximum pile distance (m)	443.59	395.64
Minimum pile cost (\$)	5.94	5.94
Average pile cost (\$)	13.64	12.53
Maximum pile cost (\$)	19.57	17.95
Harvestable cut trees		
Minimum tree volume (m ³)	0.05	0.05
Average tree volume (m ³)	0.25	0.29
Maximum tree volume (m ³)	1.71	2.64
Minimum tree cost (\$)	0.20	0.24
Average tree cost (\$)	3.71	2.75
Maximum tree cost (\$)	18.07	17.95

Table 3. Parameters used in the Fuel Reduction Cost Simulator (FRCS) to calculate skidding costs under each thinning scenarios.

FRCS parameters	Scenario I	Scenario II
Skidder rental rate (\$/hour)	85.00	85.00
Average slope (%)	13.50	13.50
Average skidding slope distance (m)	184.17	184.17
Area (ha)	4.60	4.60
Removal (trees per ha)	164.13	275.00
Average cut-tree volume (m ³)	0.25	0.29
Average cut-tree dbh (cm)	20.57	21.64
Maximum cut-tree volume (m ³)	1.71	2.64

Conclusions

Due to advanced remote sensing and GIS technologies that have brought us to an unprecedented level of precision in terrain and vegetation mapping, high-resolution DEMs and individual tree stem maps are now available for forest resource management applications. With such stem maps, silvicultural prescriptions can be developed and implemented at the individual tree level, which can potentially help meet desired management goals more effectively than the conventional way of developing and applying prescriptions. To facilitate individual tree-level decisionmaking, we have developed a cost model that estimates skidding costs for individual cut trees for thinning operations based on tree volume and locations.

Table 4. Comparison of average skidding cost results among various cost models including our individual-tree cost model, the Fuel Reduction Cost Simulator (FRCS), and six published regression models used in the FRCS for both thinning scenarios.

Skidding cost models	Skidding cost (US\$/m ³)	
	Scenario I	Scenario II
Individual-tree cost model	14.80	9.48
FRCS (Hartsough et al. 2001)	11.12	9.93
Gebhardt (1977)	5.99	5.21
Johnson (1988)	12.59	11.49
Andersson and Young (1998)	10.46	9.70
Gardner (1979)	17.16	15.33
Gibson and Egging (1973)	13.38	11.94
Johnson and Lee (1988)	14.72	13.51

The model was applied to a treatment unit where merchantable trees were to be selectively harvested under two hypothetical thinning scenarios. Comparison of the model results with those obtained from the existing cost models indicates that our model results are within a reasonable range for skidding costs but more sensitive to thinning intensities than the existing models. In addition, our model can be potentially used as a tool to develop skidding trail networks and delineate difficult terrain areas for skidding operations.

The model should be further validated through field tests to ensure that the results are applicable on the ground. There is also a need to develop appropriate cycle time regression equations for the model. The model currently uses two regression equations for uphill and downhill skidding cycle times, but they do not directly account for the effects of ground slopes, number of logs, log-pile volume, or wide range of skidding distances on cycle times. The simple skid-trail network design is another limitation of the model. Many sharp turns and skid-trail crossings exist in the optimal skid-trail network because only the second-order neighborhood system (eight adjacent grid cells) was considered. More realistic skid trails can be obtained by reducing node spacing, increasing the number of neighbor cells considered, or both. However, other skid trail design factors, such as the skidder's minimum turning radius, should also be considered for link feasibility to ensure that the skid trails identified by the model can be implemented on the ground.

Literature Cited

AGREE, J.K., AND C.N. SKINNER. 2005. Basic principles of forest fuel reduction treatments. *For. Ecol. Manag.* 211(1–2):83–96.

ANDERSON, A.E., AND J. NELSON. 2004. Projecting vector-based road networks with a shortest path algorithm. *Can. J. For. Res.* 34(7):1444–1457.

ANDERSSON, B., AND G. YOUNG. 1998. *Harvesting coastal second growth forests: Summary of harvesting system performance*. FERIC Tech. Rep. TR-120.

BAILEY, J.D., AND J.C. TAPPEINER. 1998. Effects of thinning on structural development in 40- to 100-year-old Douglas-fir stands in western Oregon. *For. Ecol. Manag.* 108(1–2):99–113.

BARBOUR, R.J., D. FAYLE, G. CHAURET, J. COOK, M.B. KARSH, AND S. RAN. 1994. Breast-height relative density and radial growth in mature jack pine (*Pinus banksiana*) for 38 years after thinning. *Can. J. For. Res.* 24(12):2439–2447.

BIESECKER, R.L., AND R.D. FIGHT. 2006. *My fuel treatment planner: A use guide*. US For. Serv. Gen. Tech. Rep. PNW-GTR-663. US For. Serv., Pac. Northw. Res. Stn., Portland, OR. 31 p.

BRODIE, J.D., D.M. ADAMS, AND C. KAO. 1978. Analysis of economic impacts on thinning and rotation for Douglas-fir using dynamic programming. *For. Sci.* 24(4):513–522.

BUSTOS-LETELIER, O. 2010. *A comparison of production, costs and stand impacts among four yarding methods*. PhD dissertation, Univ. of Maine, Orono, ME. 124 p.

CAO, T., K. HYYTIÄINEN, O. TAHVONEN, AND L. VALSTA. 2006. Effects of initial stand states on optimal thinning regime and rotation of *Picea abies* stands. *Scand. J. For. Res.* 21(5):388–398.

CAREY, A.B. 2001. Induced spatial heterogeneity in forest canopies: Response of small mammals. *J. Wildl. Manag.* 65(4):1014–1027.

CONTRERAS, M. AND W. CHUNG. 2009. Designing skid-trail networks to minimize skidding cost and soil disturbances. In *Proc. of Environmentally sound forest operations*. Council of Forest Engineering, 32nd Annual Meeting, Kings Beach, CA. Available online at frec.vt.edu/cofe/2009.htm; last accessed May 2011.

CHUNG, W., J. SESSIONS, AND H. HEINMANN. 2004. An application of heuristic network algorithm to cable logging layout design. *Int. J. For. Eng.* 15(1):11–24.

DIJKSTRA, E. 1959. A note on two problems in connexion with graphs. *Numerische Math.* 1:269–271.

FIGHT, R.D., X. ZHANG, AND B.R. HARTSOUGH. 2003. *User guide for STHARVEST: Software to estimate the cost of harvesting small timber*. US For. Serv. Gen. Tech. Rep. PNW-GTR-582. US For. Serv., Pac. Northw. Res. Stn., Portland, OR. 12 p.

GARDNER, R.B. 1979. *Turn cycle time prediction for rubber tired skidders in the northern Rockies*. US For. Serv. Res. Note INT-257. US For. Serv., Intermount. For. Range Exp. Stn., Ogden, UT. 5 p.

GEBHARDT, P.D. 1977. *Timber harvesting production rates in mixed-conifer stands of eastern Oregon and Washington*. Master of Forestry thesis, Univ. of Washington, Seattle, WA. 173 p.

GIBSON, D.F., AND L.T. EGGING. 1973. *A location model for determining the optimal number and location of decks for rubber-tires skidders*. Paper No. 73-1534. American Society of Agricultural Engineers, St. Joseph, MI.

GRAHAM, R.T., A.E. HARVEY, T.B. JAIN, AND J.R. TONN. 1999. *The effects of thinning and similar stand treatments on fire behavior in western forests*. US For. Serv. Gen. Tech. Rep. PNW-GTR-463. US For. Serv., Pac. Northw. Res. Stn., Portland, OR. 27 p.

HARTSOUGH, B.R., X. ZHANG, AND R.D. FIGHT. 2001. Harvesting cost model for small trees in natural stands in the Interior Northwest. *For. Prod. J.* 51(4):54–61.

HAN, H.-S., AND C. RENZIE. 2005. Productivity and cost of partial harvesting method to control mountain pine beetle infestation in British Columbia. *West. J. Appl. For.* 20(2):128–133.

HAYES, J.P., S.S. CHAN, W.H. EMMINGHAM, J.C. TAPPEINER, L.D. KELLOGG, AND J.D. BAILEY. 1997. Wildlife response to thinning young forests in the Pacific Northwest. *J. For.* 95(8):28–33.

HIRSCHMUGL, M., M. OFNER, J. RAGGAM, AND M. SCHARDT. 2007. Single tree detection in very high resolution remote sensing data. *Remote Sens. Environ.* 110(4):533–544.

HOF, J., AND M. BEVERS. 2000. Optimizing forest stand management with natural regeneration and single-tree choice variables. *For. Sci.* 46(2):168–175.

HOOKE, R., AND T. JEEVES. 1961. Direct search solution of numerical and statistical problems. *J. ACM* 8(2):212–219.

HYYTIÄINEN, K., O. TAHVONEN, AND L. VASTA. 2005. Optimum juvenile density, harvesting, and stand structure in even-aged Scot pine stands. *For. Sci.* 51(2):120–133.

JOHNSON, L.R. 1988. *Final report: Summary of production and timber studies of mechanized harvesting equipment in the Intermountain West*. Department of Forest Products, University of Idaho, Moscow, ID. 26 p.

JOHNSON, L.R., AND H.W. LEE. 1988. Skidding and processing of forest residues for fire-wood. *For. Prod. J.* 38(3):35–40.

KEYSER, C.E., COMP. 2010. Northern Idaho/Inland Empire (NI/IE) variants overview: Forest Vegetation Simulator. US For. Serv. Internal Rep. US For. Serv., For. Manag. Serv. Ctr., Fort Collins, CO. 49 p.

MALTAMO, M., K. MUSTONEN, J. HYYPPÄ, J. PITKÄNEN, AND X. YU. 2004. The accuracy of estimating individual tree variables with airborne laser scanning in a boreal nature reserve. *Can. J. For. Res.* 34(9):1791–1801.

MALTAMO, M., K. EERIKÄINEN, P. PACKALEN, AND J. HYYPPÄ. 2006. Estimation of stem volume using laser scanning-based canopy height metrics. *Forestry* 79(2):217–229.

PACKALEN, P., AND M. MALTAMO. 2006. Predicting the plot volume by species using airborne laser scanning and aerial photographs. *For. Sci.* 52(6):611–622.

PALAHÍ, M., AND T. PUKKALA. 2003. Optimizing the management of Scot pine (*Pinus sylvestris* L.) stands in Spain based on individual-tree models. *Ann. For. Sci.* 60:105–114.

POLLET, J., AND P.N. OMI. 2002. Effect of thinning and prescribed burning on crown fire severity in ponderosa pine forests. *Int. J. Wildl. Fire* 11(1):1–10.

POPESCU, S.C., AND R.H. WYNNE. 2004. Seeing the trees in the forest: Using LIDAR and multispectral data fusion with local filtering and variable window size for estimating tree height. *Photogramm. Eng. Remote Sens.* 70(5):589–604.

PUKKALA, T., AND J. MIINA. 1998. Tree-selection algorithm for optimizing thinning using a distance-dependent growth model. *Can. J. For. Res.* 28(5):693–702.

PUKKALA, T., AND J. MIINA. 2005. Optimizing the management of a heterogeneous stand. *Silva Fenn.* 39(4):525–538.

RAUTIAINEN, O., T. PUKKALA, AND J. MIINA. 2000. Optimising the management of even-aged *Shorea robusta* stands in Nepal using individual tree growth models. *For. Ecol. Manag.* 126(3):417–429.

- ROWELL, E., C. SEIELSTAD, L. VIERLING, L. QUEEN, AND W. SHEPPERD. 2006. Using laser altimetry-based segmentation to refine automated tree identification in managed forests of the Black Hills, South Dakota. *Photogramm. Eng. Remote Sens.* 72(12):1379–1388.
- ROWELL, E., C. SEIELSTAD, J. GOODBURN, AND L. QUEEN. 2009. Estimating plot-scale biomass in a western North American mixed-conifer forest from LiDAR-derived tree stems. In *Proc. of Silvilaser 2009: 9th international conf. on Lidar applications for assessing forest ecosystems*. Popescu, S., R. Nelson, K. Zhao, and A. Neuenschwander (Eds.). ISBN 978-1-61623-997-3. Texas A&M University, College Station, TX. 395 p.
- SHAO, G., AND K. REYNOLDS. 2006. *Computer applications in sustainable forest management: Including perspectives on collaboration and integration*. Springer-Verlag, New York, NY. 277 p.
- SURATNO, A., C. SEIELSTAD, AND L. QUEEN. 2009. Tree species identification in mixed coniferous forest using laser scanning. *J. Photogramm. Remote Sens.* 64(6):683–693.
- TAN, J. 1999. Locating forest roads by a spatial and heuristic procedure using microcomputers. *Int. J. For. Eng.* 10:91–100.
- VALSTA, L. 1992. An optimization model for Norway spruce management based on individual-tree growth models. *Acta For. Fenn.* 232.